Kinetics of Submonolayer Epitaxial Growth

Jacques G. Amar

Department of Physics & Astronomy, University of Toledo, Toledo, OH 43606

Fereydoon Family

Department of Physics, Emory University, Atlanta, GA 30322

Mihail N. Popescu

Max-Planck-Institut für Metallforschung, Heisenbergstraße 1,

D-70569 Stuttgart, Germany

Molecular beam epitaxy is an important method for growing thin-films and nanostructures. One of the scientific challenges is to understand the fundamental processes that control the evolution of thin film structure and morphology. The results of kinetic Monte Carlo simulations carried out to study the dependence of the submonolayer scaled island-size distribution on the critical island-size are presented and compared with experiments. A recently developed method which involves a self-consistent coupling of evolution equations for the capture-zone distributions with rate-equations for the island-size distribution is also described. Our method explicitly takes into account the existence of a denuded ("capture") zone around every island and the correlations between the size of an island and the corresponding average capture zone, and has been used to develop a quantitative rate-equation approach to irreversible submonolayer growth on a two-dimensional substrate. The resulting predictions for the capture-zones, capture numbers, and island-size distributions are in excellent agreement with experimental results and kinetic Monte Carlo simulations.

To appear in Computer Physics Communications, proceedings of the STATPHYS Satellite Conference: Challenges in Computational Statistical Physics in the 21st Century
(July 30, 2001)

I. Introduction

Molecular beam epitaxy (MBE) is one of the most effective techniques for growing high purity materials including a variety of semiconductors and magnetic materials for applications in electronic and optoelectronic devices [1,2]. In this method a constant flux of atoms impinge under ultrahigh vaccuum conditions on a substrate held at a fixed temperature to grow a high quality crystalline material. The long-standing scientific challenge in this area has been to model epitaxial growth conditions and understand what are the fundamental processes that control the evolution of epitaxial structure and morphology.

The fundamental physical processes in the growth of thin films by molecular beam epitaxy involve nucleation, aggregation and coalescence of islands on a two-dimensional substrate [1] - [3]. In the submonolayer and early multilayer regime this leads to the formation of a distribution of islands of various sizes and morphologies which grow and coalesce with time. The island-size distribution exhibits a general dynamic scaling behavior, similar to that observed in aggregation [4] and vapor-deposited thin-film growth [5,6], but the island morphology depends on the microscopic details of the growth process such as the deposition rate, temperature, island-relaxation mechanisms and the structure of the substrate.

The scaling behavior in the submonolayer is important for a variety of reasons. For example, the experimental and theoretical study of the scaling behavior of the island-density and distribution in the submonolayer regime may be used to determine a variety of important microscopic parameters in epitaxial growth. In particular, a study of the scaling of the island density as a function of deposition rate and temperature, has enabled the determination of such quantities as the activation energy for monomer diffusion as well as the critical island size for island nucleation in a variety of systems [7] - [19].

In addition, the submonolayer regime has important consequences for multilayer growth. For example, due to the existence in many systems of a so-called Ehrlich-Schwoebel (ES) barrier for interlayer diffusion [20], i.e. an additional barrier beyond that for normal diffusion for atoms to hop down from the edge of an island, the quality of multilayer film growth may be strongly affected by the island-distribution and morphology in the submonolayer

[12,21]. In particular, the effects of the barrier, combined with the island-size distribution and morphology, may determine whether growth is "layer-by-layer" or three-dimensional. As an example, the reentrant RHEED oscillations which occur with decreasing temperature in Pt/Pt(111) growth have been shown [22,23] to be due to a change in island morphology with decreasing temperature combined with the existence of a finite barrier for hopping down a step. As another example, the addition of impurities on a surface has recently been shown [12] to lead to improved layer-by-layer growth, since the increased island density due to heterogeneous nucleation leads to a reduced island size thus promoting interlayer diffusion.

This paper is a review of some of the recent progress that has been made in understanding submonolayer epitaxial growth. The organization of the paper is as follows. In Section II, we introduce the concept of critical island size and discuss the general rate-equation theory and scaling in submonolayer epitaxial growth. As already mentioned, an understanding of submonolayer growth is important not only in explaining the microscopic mechanisms involved in island growth and nucleation, but also in understanding the various growth modes involved in later multilayer growth and in surface roughening. In Section III, we present the results of kinetic Monte Carlo simulations for the scaled island-size distribution as a function of critical island size and compare with experiments. In Section IV, we present a new self-consistent rate-equation approach to island-size distributions for the case of irreversible growth. Finally, we present our conclusions in Section V.

II. Rate Equation Theory and Scaling of the Island-Size Distribution

The fundamental quantity in the kinetic description of island growth is the island size distribution function $N_s(t)$, which gives the density of islands of size s (where s is the number of atoms or particles in the island) at time t. The traditional method for studying the kinetics of cluster growth processes is based on the theoretical approach developed by Smoluchowski [24] who wrote down an equation for the evolution of the cluster size distribution using a mean-field argument which neglects fluctuations and geometry. For the case in which only monomers diffuse, one can write down a simple set of equations [25,26] governing the density of monomers N_1 and the density $N_s(t)$ of islands of size s at time t. Including dissociation

but ignoring both coalescence and the contribution to island growth due to arriving adatoms landing directly on top of an island, one has generally,

$$\frac{dN_1}{dt} = F - 2\sigma_1 D N_1^2 - N_1 D \sum_{s\geq 2} \sigma_s N_s + \sum_{s>1} \gamma_s N_s \tag{1}$$

$$\frac{dN_s}{dt} = N_1 D(\sigma_{s-1} N_{s-1} - \sigma_s N_s) - \gamma_s N_s + \gamma_{s+1} N_{s+1} \quad (s > 1) \tag{2}$$

where D is the monomer diffusion rate, F is the deposition rate, and the σ_s (γ_s) govern the rate of attachment (detachment) of adatoms on the substrate from islands of size s. The first three terms on the right of Eq. 1 correspond to the processes of monomer deposition, monomer capture by the formation of dimers, and monomer attachment to islands respectively, while the fourth term corresponds to the rate at which monomers detach from existing islands. Similarly, the first term in parentheses on the right of Eq. 2 corresponds to the rate at which islands of size $s-1$ are converted to islands of size s by addition of monomers, while the second term corresponds to the creation of islands of size $s+1$ by addition of monomers to islands of size s, and the last two terms account for similar conversions due to detachment of monomers.

While the dependence of γ_s on island size s may be quite complicated, in general one assumes, in analogy with nucleation theory, [25,26] that there exists a critical island size i, such that islands of size larger than i are more likely to grow than to shrink, while islands smaller than i are more likely to break up. More simply, one may assume that $\gamma_s = 0$ for $s > i$, so that i corresponds to one less than the size of the smallest stable island. Then the solution of the rate-equations involves simply the knowledge of the detachment rates γ_s for $s < i$ as well as the (average) capture numbers σ_s.

Since the coverage $\theta = Ft$ is often more convenient for comparison with experiments, we express the time dependence of the island size distribution and its moments in terms of θ. Defining the total island density N (excluding monomers) and the coverage θ by,

$$N = \sum_{s\geq 2} N_s(\theta) \quad \text{and} \quad \theta = \sum_{s\geq 1} s N_s, \tag{3}$$

then the average island size S can be written in terms of the zeroth and first moments as, [27,28]

$$S = \frac{\sum_{s\geq 2} sN_s(\theta)}{\sum_{s\geq 2} N_s(\theta)} = \frac{(\theta - N_1)}{N} \tag{4}$$

where N_1 is the monomer density.

According to the dynamic scaling assumption [4] there exists only one characteristic size in the problem which is the mean island size $S(\theta)$ defined in (3). This implies that $N_s(\theta)$ scales with $S(\theta)$ and one may write generally $N_s(\theta) = A(S,\theta) f_i(s/S)$, where $f_i(u)$ is the scaling function for the island size distribution corresponding to the case in which the value of the critical island size is equal to i. Using the definition of θ and the scaling form for the island-size distribution one can write, $\theta = \sum_{s\geq 1} sN_s(\theta) = A(S,\theta)S^2 \int_0^\infty f_i(u)udu$ which implies $A(S,\theta) \sim \theta/S^2$. Taking $A(S,\theta) = \theta/S^2$, one may write the general scaling form [5], [27]- [33],

$$N_s(\theta) = \theta\ S^{-2} f_i(s/S). \quad (s \geq 2) \tag{5}$$

where the scaling function $f_i(u)$ satisfies,

$$\int_0^\infty f_i(u)\ u\ du = 1 \tag{6}$$

where $f_i(u) \sim u^{\omega_i}$ for $u << 1$. At late time, one expects the monomer density N_1 to be much smaller than the coverage θ so that in the scaling regime $N_1 << \theta$ and $S \simeq \theta/N$. This implies the scaling relation, $N \simeq \theta/S$, which leads to the additional sum-rule,

$$\int_0^\infty f_i(u)\ du = 1 \tag{7}$$

Using the sum-rules (6) and (7), along with the assumption that $\omega_i = i$, and that $f_i(u)$ has a peak at $u = 1$, we have derived an approximate expression for the scaling function $f_i(u)$ of the form [31],

$$f_i(u) = C_i u^i e^{-ia_i u^{1/a_i}} \tag{8}$$

where the constants C_i and a_i satisfy the expressions,

$$\frac{,\,[(i+2)a_i]}{,\,[(i+1)a_i]} = (ia_i)^{a_i} \qquad C_i = \frac{(ia_i)^{(i+1)a_i}}{a_i,\,[(i+1)a_i]} \tag{9}$$

III. Model and Simulations

In order to investigate the scaling behavior of the submonolayer island density and size-distribution as a function of critical island size i, we have studied [31] - [35] a simplified model in which atoms are randomly deposited at a rate F per site per unit time onto a regular (square or triangular) lattice while monomers, including those deposited on top of existing islands, are assumed to diffuse at the rate $D = D_0 e^{-E_a/k_B T}$ in units of nearest-neighbor hops per unit time. In our model a monomer becomes stable when it has at least z nearest-neighbors, so that the critical island size i depends on both the underlying lattice and z (see Fig. 1). For atoms which have $0 < n < z$ nearest-neighbor surface atoms, we assume that the activation energy for diffusion is given by E_n so that the relative diffusion rate is given by $r_n = D_n/D = e^{-\Delta E_n/k_B T}$ where $\Delta E_n = E_n - E_a$. In order to study the effects of edge-diffusion on island morphology we have also included an additional parameter $r_e = e^{-\Delta E_e/k_B T}$ corresponding to diffusion of atoms with one-nearest neighbor (i.e. "1-bond diffusion") along the edge of an island. By varying r_n, r_e, and z and studying various lattices, we have studied the island-size distribution, density, and morphology for $i = 0, 1, 2$ and 3.

Fig. 2 (a) shows our kinetic Monte Carlo results for the island-size distribution scaling function for the case $i = 1$, obtained from simulations of extended islands on square and triangular lattices with $z = 1$, corresponding to deposition with irreversible nearest-neighbor attachment. The open circles and triangles correspond to simulations without edge-diffusion, which leads to fractal islands, while the open diamonds correspond to simulations of compact square islands with finite edge-diffusion. Also shown (solid curve) is the approximate expression (8) for $f_1(u)$, along with experimental results for Fe/Fe(100) deposition in the temperature range 20^o C - 207^o C [13]. As can be seen, there is good agreement between our simulation results and the approximate analytical form (8) as well as with the Fe/Fe(100) experimental results. We note however, that the island-size distribution scaling function $f_1(u)$ appears to depend on the island morphology for small u [31], [35], since for fractal

islands $f_1(0)$ appears to approach zero at finite coverage with increasing D/F [35], while for compact islands $f_1(0)$ remains finite, in contrast to the prediction of Eq. 8.

The case $i = 2$, for which the minimal stable island is a trimer, was simulated using a simple model on a triangular lattice in which any atom with two or more nearest-neighbors is irreversibly 'frozen' (i.e. $z = 2$). The additional activation energy ΔE_1 for an atom which has only one bond is taken to be finite. Figure 2 (b) shows our simulation results for the island-size distribution scaling function for $i = 2$ with $D/F = 10^7 - 10^8$, $\theta = 0.1 - 0.4$ for $r_1 = 0.003, 0.05$, and 1. Also shown is the approximate analytic form (8) for $f_2(u)$ which agrees quite well with our simulation results.

The case $i = 3$ has been suggested as the critical cluster size for Fe/Fe (100) deposition at elevated temperatures [14] since at these temperatures the probability of one-bond detachment becomes significant while the probability of two-bond detachment is negligible. In this case the minimal stable configuration is a tetramer (see Fig. 1) and we have studied a similar model as for $i = 2$ but on a square lattice. As can be seen in Fig. 2(c) the simulation results (both with and without enhanced edge diffusion) cover a wide range of coverages as well as values of D/F and r_1. There is again very good agreement between all our simulation results and the approximate analytical form (8) as well as the experiments. Finally, we note that the case $i = 0$, which corresponds to the spontaneous nucleation or 'freezing' of monomers has also been studied by kinetic Monte Carlo simulations [31], [34] and good agreement with experiments [16] has been found.

IV. Self-Consistent Rate-Equation Approach to Island-Size Distributions

While the scaled island-size distributions may be calculated via kinetic Monte Carlo simulations as discussed above, and are reasonably well approximated for extended islands using the approximate form (8), we would like to be able to predict the scaled distributions $f_i(u)$ as a function of the critical island size i from first-principles. Unfortunately, even for the case of irreversible growth ($i = 1$), use of the rate-equation approach with simple choices for the capture numbers σ_s (i.e. $\sigma_s \sim s^p$ with $0 \leq p \leq 1/2$) leads to a scaled island-size distribution function which diverges in the limit of large D/F [27], [31], [36].

Similarly, while a self-consistent rate-equation (RE) approach has recently been developed [37] which can quantitatively predict *average* quantities such as the total island density $N(\theta)$ and monomer density $N_1(\theta)$ in the pre-coalescence regime, such an approach does not lead to correct predictions for the island-size distributions. Self-consistent rate-equation results for the island density and monomer density have also been obtained for one-dimensional growth [38] and for reversible two-dimensional growth [39]. However, in all cases the island-size distributions are not correctly predicted. The reason is that spatial and temporal correlations in the growth of islands [40–42] are neglected in these approaches.

Here we review a novel calculation scheme [43] which captures the essential correlations between the size of the island, the corresponding average capture zone, and the capture number. A second set of equations, coupled to the usual rate-equations, is used to describe the evolution of the island-size dependent capture zones. The combined set of equations leads to size- and coverage-dependent capture numbers $\sigma_s(\theta)$ in good agreement with experimental [41] and kinetic Monte Carlo (KMC) simulation results [27]. Furthermore, numerical integration of the island-density rate-equations with these capture numbers leads to island-size distributions in good agreement with KMC simulations.

IV.A. Rate-equations for irreversible growth

Dividing Eqs. (1) and (2) by the deposition rate F, and including the effects of atoms landing directly on islands, the RE's for irreversible growth may be written,

$$\frac{dN_1}{d\theta} = \gamma - 2N_1 - 2R\sigma_1 N_1^2 - RN_1 \sum_{s\geq 2} \sigma_s N_s \tag{10}$$

$$\frac{dN_s}{d\theta} = RN_1 \left(\sigma_{s-1}N_{s-1} - \sigma_s N_s\right) + k_{s-1}N_{s-1} - k_s N_s, \quad \text{for } s \geq 2, \tag{11}$$

where θ is the coverage and γ is the fraction of the substrate not covered by islands. Here, the kinetic constant $R = D/F$ is the ratio of the diffusion constant D to the deposition flux F, where $D = D_h/4$ for the case of isotropic nearest-neighbor hopping with rate D_h on a two-dimensional isotropic square lattice. The terms with σ_s describe the rate of monomer capture by other monomers or by existing islands, while the terms with k_s (where $k_s = s^{2/d_f}$

and d_f is the fractal dimension of the islands [37]) correspond to the deposition of adatoms directly on islands of size s.

IV.B. Monomer Diffusion and Local Capture Numbers

In what follows we restrict the discussion to the case of two-dimensional growth, but our approach may also be extended to one-dimensional growth [43], [44]. In order to take into account the correlation between an island and its local capture zone, we consider the following model for the environment of an island. An island of size s is approximated by a circular region of radius $R_s = \rho\ s^{1/d_f}$, where ρ is a "geometrical" prefactor which accounts for the circular approximation of the island area while the fractal dimension d_f depends on the morphology of the island. The area surrounding the island is divided into an inner ($R_s < r < R_{ex}$) and an outer region ($R_{ex} < r < \infty$). The inner region corresponds to an "exclusion" zone in which only monomers can be found. The area of the exclusion zone A_{ex} is assumed to be proportional to the area A of the Voronoi polygon surrounding the island, i.e. $A_{ex} = \eta A$ where the factor η (typically larger than 1) is assumed to be the same for all islands. Accordingly, the radius of this zone is $R_{ex} = \sqrt{\eta}\ R$, where $R = \sqrt{A/\pi}$ is the "radius" of the Voronoi polygon. In the outer region, corresponding to $r > R_{ex}$, we assume a "smeared" uniform distribution of monomers and islands which is independent of the size of the central island, as in Ref. [37].

This geometry naturally leads to the definition of a mean-field "nucleation" length $\xi_1 = 1/\sqrt{2\sigma_1 N_1}$ and to that of a monomer "capture" length $\xi = (2\sigma_1 N_1 + \sum_{s\geq 2} \sigma_s N_s)^{-1/2}$. In terms of these quantities, and defining $\alpha = \xi_1/\xi$, one can obtain the following quasistatic diffusion equation [45] satisfied by the local monomer density,

$$\nabla^2 n_1 \simeq \begin{cases} \xi_1^{-2}(n_1 - \alpha^2(N_1/\gamma)), & \text{for } R_s < r \leq R_{ex}, \\ \xi^{-2}(n_1 - N_1/\gamma), & \text{for } r > R_{ex}. \end{cases} \tag{12}$$

The explicit solution of Eq. (12), with appropriate boundary conditions for irreversible growth, is used to determine the local capture number $\tilde{\sigma}_s(A) = (2\pi R_s/N_1)(\partial n_1/\partial r)_{R_s}$ for $s \geq 2$. The monomer capture number σ_1 is also obtained by taking the limit of no exclusion zone, i.e. $R_{ex} = R_1$. After choosing a reasonable value for ρ, the decay length ξ and the

geometrical prefactor η are self-consistently obtained by requiring that the capture-number condition, $\xi^{-2} = \xi_1^{-2} + \sum_{s\geq 2} \sigma_s N_s$ and monomer-density condition that the average monomer density in all the Voronoi cells must equal N_1, are satisfied at all coverages [45].

IV.C. Voronoi Area Distribution Evolution Equations

In order to compute the capture numbers $\sigma_s = \langle \tilde{\sigma}_s(A) \rangle_{G_s(A)}$, one has to determine the Voronoi-area distribution $G_s(\theta; A)$, where $G_s(\theta; A)$ is the number density (per site) of islands of size s surrounded by a Voronoi cell of area A. Taking into account the change in the areas by nucleation and aggregation of islands, and ignoring for the moment the break-up of Voronoi areas when new islands are nucleated, one can write a general set of evolution equations for the functions $G_s(\theta; A)$ in the following form,

$$\frac{dG_2(\theta; A)}{d\theta} = (dN/d\theta)\ \delta(A - A_{av}) - RN_1 \tilde{\sigma}_2(A) G_2(\theta; A), \tag{13}$$

$$\frac{dG_s(\theta; A)}{d\theta} = RN_1\ [\tilde{\sigma}_{s-1}(A) G_{s-1}(\theta; A) - \tilde{\sigma}_s(A) G_s(\theta; A)] \quad (s \geq 3). \tag{14}$$

The first term on the right side of (13) corresponds to nucleation of dimers while the remaining terms in (13) and (14) correspond to growth of islands via aggregation. It has been assumed that the Voronoi areas around the (new) dimers nucleated at coverage θ are equal to the average Voronoi area at that coverage, $A_{av} = 1/N$. The break-up of larger areas due to nucleation, neglected in (14), will be accounted for through a uniform rescaling to be justified *a posteriori*.

In principle, Eqs. (13) and (14) can be numerically integrated. However, if the local capture number $\tilde{\sigma}_s(A)$ has no explicit dependence on the island-size s (as in the case of point islands), then an analytic solution can be obtained. We therefore consider the mean-field approximation $\tilde{\sigma}_s(A) \simeq \tilde{\sigma}_S(A)$ (where $S = (\theta - N_1)/N$ is the average island size). After changing the coverage variable to $x_A = \int_{\theta_A}^{\theta} R\ N_1(\phi)\ \tilde{\sigma}_S(A)\ d\phi$ (where $1/N(\theta_A) = A$ defines θ_A), (13) and (14) can be solved in closed form [43],

$$G_s(x_A; A) = B_A\ x_A^{s-2}\ e^{-x_A}/(s-2)! \quad (s \geq 2). \tag{15}$$

In the aggregation regime Eq. (15) corresponds to a sharply peaked distribution as a function of A whose peak position $\hat{A}_s$ satisfies

$$x_{\hat{A}_s} = s - 2, \tag{16}$$

and, using the appropriate expression for the local capture number $\tilde{\sigma}_s(A)$, one can approximate $\sigma_s = \tilde{\sigma}_s(\hat{A}_s)$.

Because the effects of break-up of Voronoi cells due to nucleation have been neglected in (13) and (14), the Voronoi areas $\hat{A}_s$ must be rescaled so that the average Voronoi area is equal to $A_{av} = 1/N$ as described in detail in [43,45] (in the case of extended islands additional geometrical corrections are included). Accordingly, the capture numbers are approximated by $\sigma_s = \tilde{\sigma}_s(A'_s)$ where A'_s is the rescaled and corrected $\hat{A}_s$.

IV.D. Results

We have numerically integrated the island-density rate-equations (10) - (11) coupled with the solution of the Voronoi-area evolution equations (13) - (14) as described above, in order to calculate the scaled island-size distributions $f(s/S) = (S^2/\theta)\ N_s(\theta)$ and scaled capture-number and capture-zone distributions for the case of irreversible growth on both one- and two-dimensional substrates. Fig. 3 shows typical results for the case of compact islands ($d_f = 2$) in two-dimensions. As can be seen in Fig. 3(a), there is excellent agreement between the calculated scaled island-size distribution $f(s/S)$ (solid line) and kinetic Monte Carlo simulations (symbols), in contrast to the corresponding mean-field (MF) prediction (dashed line). Our RE predictions for the capture-number distribution for compact islands are also in very good agreement with experimental results for two different materials and growth conditions from Ref. [41] as shown in Fig. 3(b). The reason for this is that the explicit inclusion of size correlations in the rate equations has led to correct expressions for the capture zones and capture numbers. Similar good agreement with simulations has also been obtained [43], [45] for both point and fractal islands in two-dimensions, as well as for both point and extended islands in one-dimension [44], although in the latter case the details of the calculation of the capture zones and numbers are somewhat different due to

the existence of strong spatial fluctuations.

V. Conclusions

Over the past few years great progress has been made in our understanding of epitaxial growth using simple realistic models as well as scaling ideas and rate-equation analyses. This has led to a good quantitative explanation of a number of recent experiments in submonolayer growth (for a review see Ref. [46]). For example, the role of the critical island size and its variation with deposition rate and temperature has been shown to be crucial in determining the island-size distribution and morphology in submonolayer growth. In particular, we have shown that our simulation results for the scaled island-size distribution give very good agreement with experiments corresponding to critical island sizes $i = 0 - 3$. By using a self-consistent rate-equation approach in which the existence of a denuded ("capture") zone around every island and the correlations between the size of the island and the corresponding average capture zone are explicitly taken into account, we have also obtained rate-equation results for the island size-distribution, capture zones, and capture numbers in very good agreement with experimental results and kinetic Monte Carlo simulations for the case of irreversible growth.

Future studies of both submonolayer and multilayer growth will focus on a more detailed understanding of the effects of microscopic interactions using more realistic models. Of particular interest are the effects of small-cluster diffusion and many-body interactions on the island density scaling behavior and on the island-size distribution. We note that it should be possible to extend the coupled rate-equation method presented here to the case of reversible growth, in order to predict the scaled island-size distribution as a function of the critical island size i. We also expect that the basic idea of coupled evolution of the capture-zones and island densities included in our approach may be used in the rate-equation modeling of a wide variety of problems involving cluster nucleation and growth by aggregation.

REFERENCES

[1] J. Y. Tsao, *Materials fundamentals of molecular beam epitaxy*, World-Scientific, Singapore, 1993.

[2] J. W. Matthews, *Epitaxial growth*, Academic, New York, 1975.

[3] B. Lewis and J. C. Anderson, *Nucleation and growth of thin films*, Academic, New York, 1978.

[4] T. Vicsek and F. Family, Phys. Rev. Lett. **52**, 1669 (1984).

[5] F. Family and P. Meakin, Phys. Rev. Lett. **61**, 428 (1988).

[6] F. Family and P. Meakin, Phys. Rev. A **40**, 1998 (1989) 3836.

[7] Y.W. Mo, J. Kleiner, M.B. Webb, M.G. Lagally, Phys. Rev. Lett., **66** (1991).

[8] H.J. Ernst, F. Fabre, and J. Lapujoulade, Phys. Rev. B **46**, 1929 (1992).

[9] R.Q. Hwang, J. Schroder, C. Gunther, and R.J. Behm, Phys. Rev. Lett. **67**, 3279 (1991) ; R.Q. Hwang and R.J. Behm, J. Vac. Sci. Technol. B **10**, 256 (1992).

[10] W. Li, G. Vidali, and O. Biham, Phys. Rev. B **48**, 8336 (1993).

[11] E. Kopatzki, S. Gunther, W. Nichtl-Pecher, and R.J. Behm, Surf. Sci. **284**, 154 (1993).

[12] G. Rosenfeld, R. Servaty, C. Teichert, B. Poelsema, and G. Comsa, Phys. Rev. Lett. **71**, 895 (1993).

[13] J.A. Stroscio, D.T. Pierce, and R.A. Dragoset, Phys. Rev. Lett. **70**, 3615 (1993).

[14] J.A. Stroscio and D.T. Pierce, Phys. Rev. B **49**, 8522 (1994).

[15] J.-K. Zuo and J.F. Wendelken, Phys. Rev. Lett. **66**, 2227 (1991); J.-K. Zuo, J.F. Wendelken, H. Durr, and C.-L. Liu, Phys. Rev. Lett. **72**, 3064 (1994).

[16] D.D. Chambliss and R.J. Wilson, J. Vac. Sci. Technol. **B9**, 928 (1991); D.D. Chambliss and K.E. Johnson, Phys. Rev. B **50**, 5012 (1994).

[17] K. Bromann, H. Brune, H. Roder, and K. Kern, Phys. Rev. Lett. **75**, 677 (1995).

[18] Q. Jiang and G.C. Wang, Surf. Sci. **324**, 357 (1995).

[19] F. Tsui, J. Wellman, C. Uher, and R. Clarke, Phys. Rev. Lett. **76**, 3164 (1996).

[20] G. Ehrlich and F. Hudda, J. Chem. Phys. **44**, 1039 (1966); R.L. Schwoebel, J. Appl. Phys. **40**, 614 (1969).

[21] J. Tersoff, A.W. Denier van der Gon, and R.M. Tromp, Phys. Rev. Lett. **72**, 266 (1994).

[22] R. Kunkel, B. Poelsema, L.K. Verheij and G. Comsa, Phys.

[23] P. Smilauer and D. D. Vvedensky, Phys. Rev. B **48**, 17603 (1993).

[24] M. von Smoluchowski, Z. Phys. Chem. **17**, 557 (1916); M. von Smoluchowski, Z. Phys. Chem. **92**, 129 (1917).

[25] S. Stoyanov and D. Kashchiev, in E. Kaldis (ed.), *Current Topics in Materials Science*, Vol. 7, North-Holland, Amsterdam, 1981, pp. 69-141.

[26] J.A. Venables, G.D. Spiller, and M. Hanbucken, *Rep. Prog. Phys.* **47**, 399 (1984); J.A. Venables, *Philos. Mag.* **27**, 697 (1973); *Phys. Rev. B* **36**, 4153 (1987).

[27] M.C. Bartelt and J.W.Evans, *Phys. Rev. B* **46**, 12675 (1992); M.C. Bartelt and J.W. Evans, *J. Vac. Sci. Tech. A* **12**, 1800 (1994).

[28] J.G. Amar, F. Family, and P.-M. Lam, Phys. Rev. B **50**, 8781 (1994).

[29] C. Ratsch, A. Zangwill, P. Smilauer, and D.D. Vvedensky, Phys. Rev. Lett. **72**, 3194 (1994); C. Ratsch, P. Smilauer, A. Zangwill, and D.D. Vvedensky, Surf. Sci. **328**, L599 (1995).

[30] M. Schroeder and D.E. Wolf, Phys. Rev. Lett. **74**, 2062 (1995).

[31] J.G. Amar and F. Family, Phys. Rev. Lett. **74**, 2066 (1995).

[32] F. Family and J.G. Amar, Mat. Sci. and Eng. B (Solid State Materials), **30**, 149 (1995).

[33] J.G. Amar and F. Family, Thin Solid Films **272**, 208 (1996).

[34] A. Zangwill and E. Kaxiras, Surf. Sci. **326**, L483 (1995).

[35] J.G. Amar and F. Family, in *Fractal Aspects of Materials*, MRS Symposia Proceedings No. 367, p. 241, Materials Research Society, Pittsburgh, 1995.

[36] D.D. Vvedensky, *Phys. Rev. B.* **62**, 15435 (2000).

[37] G.S. Bales and D.C. Chrzan, *Phys. Rev. B* **50**, 6057 (1994).

[38] J.A. Blackman and P.A. Mulheran, *Phys. Rev. B* **54**, 11681 (1996); P.A. Mulheran and J.A. Blackman, *Surf. Sci.* **376**, 403 (1997).

[39] G.S. Bales and A. Zangwill, *Phys. Rev. B* **55**, 1973 (1997); M.N. Popescu, J.G. Amar, and F. Family, *Phys. Rev. B* **58**, 1613 (1998).

[40] M.C. Bartelt and J.W. Evans, *Phys. Rev. B* **54**, R17359 (1996).

[41] M.C. Bartelt, A.K. Schmid, J.W. Evans, and R.Q. Hwang, *Phys. Rev. Lett.* **81**, 1901 (1998); M.C. Bartelt, C.R. Stoldt, C.J. Jenks, P.A. Thiel, and J.W. Evans, *Phys. Rev. B* **59**, 3125 (1999).

[42] P.A. Mulheran and J.A. Blackman, *Philos. Mag. Lett.* **72**, 55 (1995).

[43] J.G. Amar, M.N. Popescu, and F. Family, *Phys. Rev. Lett.* **86**, 3092 (2001).

[44] J.G. Amar, M.N. Popescu, and F. Family, to appear in Surface Science.

[45] M.N. Popescu, J.G. Amar, and F. Family, to appear in *Phys. Rev. B.*

[46] H. Brune, Surf. Sci. Rep. **31**, 121 (1998).

Figure Captions

Fig. 1: Diagram showing stable island configurations for different critical island sizes $i = 0$ to 3. The case $z = 1$ corresponds to $i = 1$ on any lattice, while $z = 2$ corresponds to $i = 2$ and 3 on triangular and square lattices respectively. Also shown is the case $i = 0$ which corresponds to freezing of monomers.

Fig. 2: Comparison of kinetic Monte Carlo simulation results (open symbols), Eq. 8 (solid line), and experimental results for Fe/Fe(100) (filled symbols) for the island-size distribution scaling function $f_i(u)$ for $i = 1, 2$, and 3. (a) $i = 1$. Simulation results are for $\theta = 0.1 - 0.4$ with $r_1 = 0$, $R = 10^8 - 10^9$, and $r_e = 0 - 10^{-4}$. Experimental data [14] are for T = 20 ^{o}C - 207 ^{o}C. (b) $i = 2$. Simulation results are for $\theta = 0.1 - 0.4$, $R = 10^7 - 10^8$, and $r_1 = 0.003 - 1$. (c) $i = 3$. Simulation results on a square lattice for $\theta = 0.06 - 0.3$ with $R = 5 \times 10^9 - 10^{11}$, $r_1 = 10^{-4} - 2.5 \times 10^{-6}$, and $r_e = 0 - 10^{-2}$. Experimental results are for $T = 301^o$C (diamonds) and $T = 356^o$C (circles).

Fig. 3: Scaled island-size and capture-number distributions for compact islands on a two-dimensional substrate ($R = 0.25 \times 10^8$). Open symbols in (b) are experimental results from [41] for Cu/Co on Ru(0001) (diamonds) and for Ag/Ag(100) (circles).

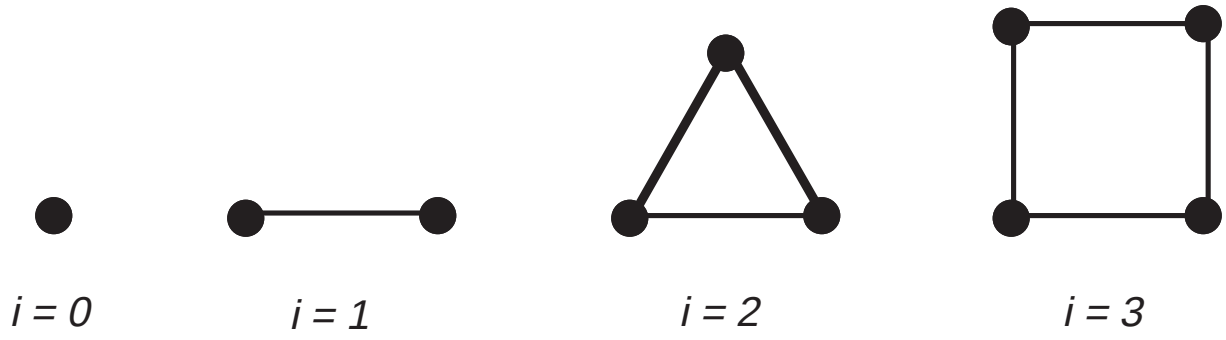

Figure 1

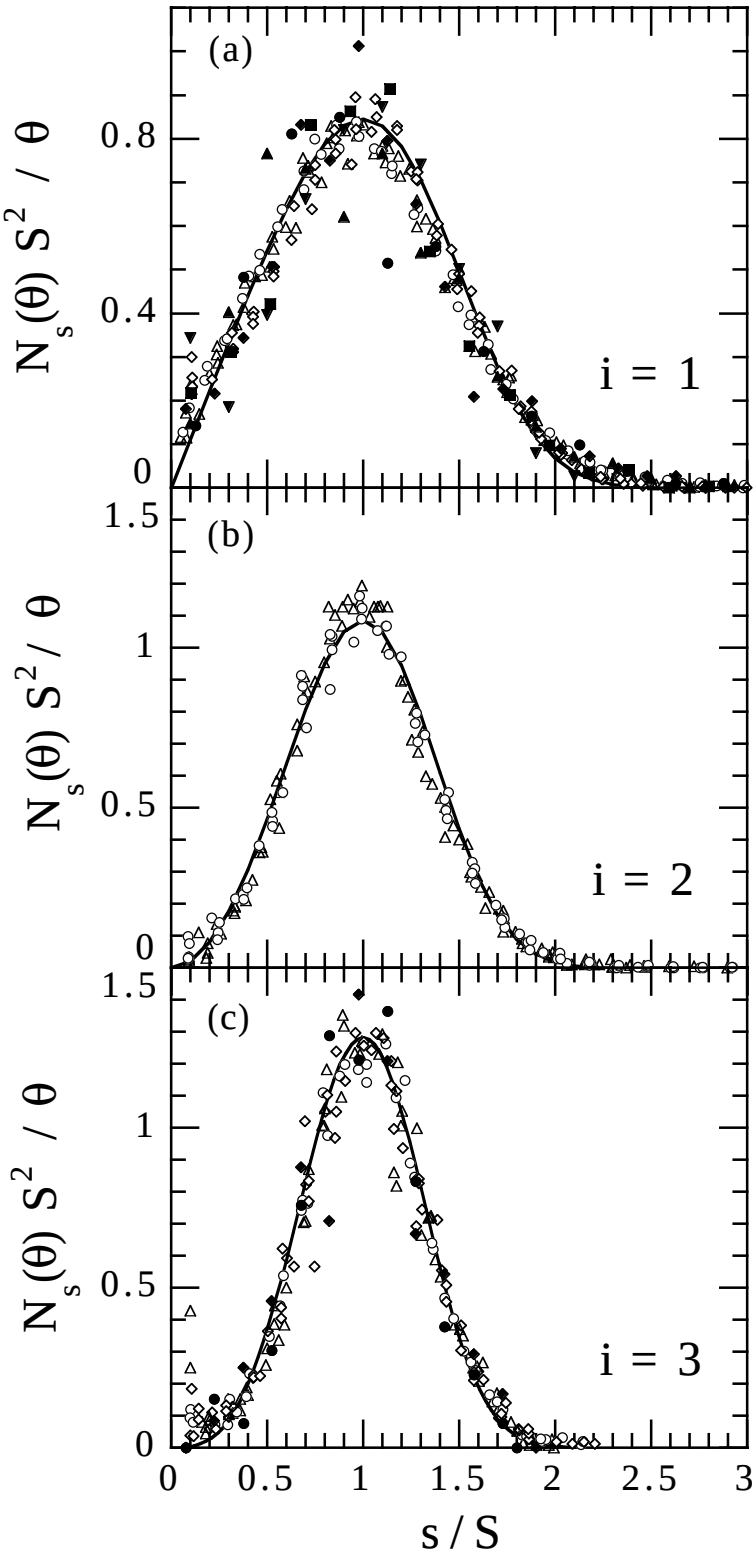

Figure 2

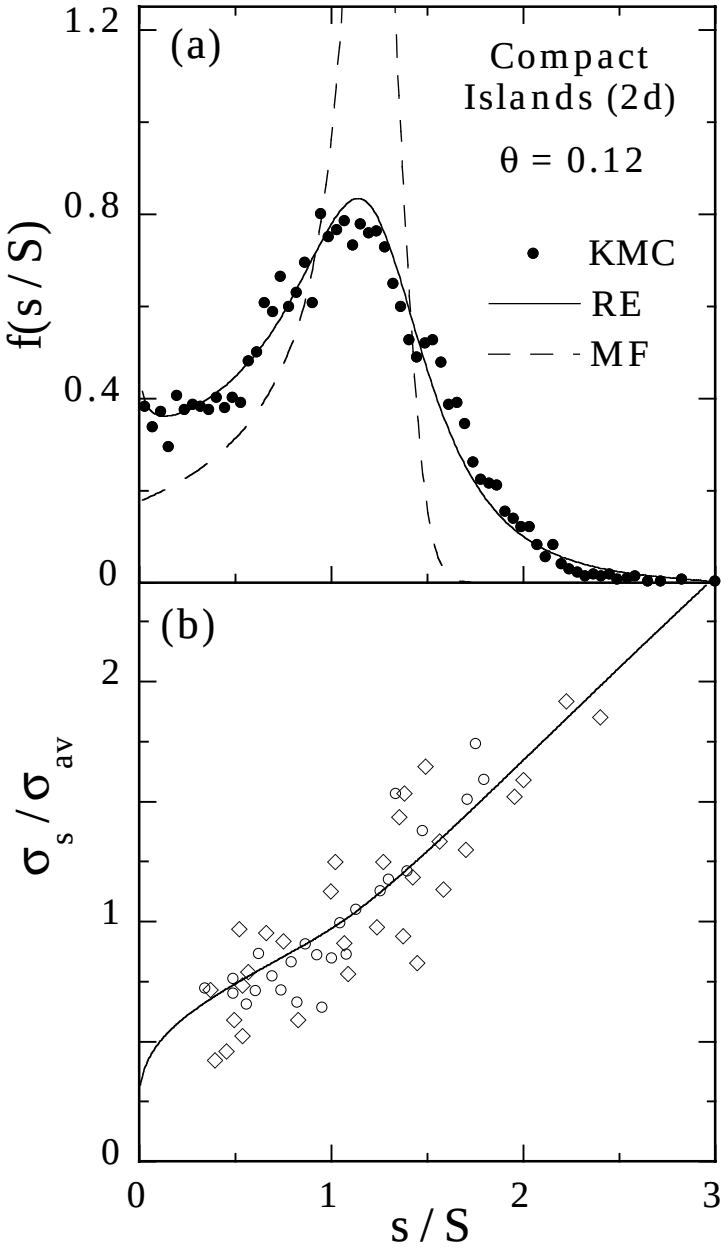
(a)
Compact
Islands (2d)
θ = 0.12
KMC
RE
MF
f(s / S)
1.2
0.8
0.4
0
(b)
σ_s / σ_av
2
1
0
0
1
2
3
s / S

Figure 3